J Arid Land (2023) 15(11): 1355–1375
https://doi.org/10.1007/s40333-023-0111-7

Science Press Springer-Verlag

Multiple assessments, source determination, and health risk apportionment of heavy metal(loid)s in the groundwater of the Shule River Basin in northwestern China

WEN Xiaohu[1], LI Leiming[2*], WU Jun[3], LU Jian[4], SHENG Danrui[1]

[1] Key Laboratory of Ecological Safety and Sustainable Development in Arid Lands, Northwest Institute of Eco-Environment and Resources, Chinese Academy of Sciences, Lanzhou 730000, China;
[2] Key Laboratory of Comprehensive and Highly Efficient Utilization of Salt Lake Resources, Qinghai Institute of Salt Lakes, Chinese Academy of Sciences, Xining 810008, China;
[3] Yantai Research Institute, Harbin Engineering University, Yantai 264006, China;
[4] Shandong Key Laboratory of Coastal Environmental Processes/CAS Key Laboratory of Coastal Environmental Processes and Ecological Remediation, Chinese Academy of Sciences, Yantai 264003, China

Abstract: Global ecosystems and public health have been greatly impacted by the accumulation of heavy metal(loid)s in water. Source-specific risk apportionment is needed to prevent and manage potential groundwater contamination with heavy metal(loid)s. The heavy metal(loid)s contamination status, water quality, ecological risk, and health risk apportionment of the Shule River Basin groundwater are poorly understood. Therefore, field sampling was performed to explore the water quality and risk of heavy metal(loid)s in the groundwater of the Shule River Basin in northwestern China. A total of 96 samples were collected from the study area to acquire data for water quality and heavy metal(loid)s risk. There was noticeable accumulation of ferrum in the groundwater of the Shule River Basin. The levels of pollution were considered to be moderately low, as evaluated by the degree of contamination, heavy metal evaluation index, heavy metal pollution index, and Nemerow pollution index. The ecological risks were also low. However, an assessment of the water quality index revealed that only 58.34% of the groundwater samples had good water quality. The absolute principal component scores-multiple linear regression model was more suited for this study area than the positive matrix factorization model. There were no obvious noncarcinogenic or carcinogenic concerns for all types of receptors according to the values of the total hazard index and total carcinogenic risk. The human activities and the initial geological environment factor (65.85%) was the major source of noncarcinogenic risk (residential children: 87.56%; residential adults: 87.52%; recreational children: 86.77%; and recreational adults: 85.42%), while the industrial activity factor (16.36%) was the major source of carcinogenic risk (residential receptors: 87.96%; and recreational receptors: 68.73%). These findings provide fundamental and crucial information for reducing the health issues caused by heavy metal(loid)s contamination of groundwater in arid areas.

Keywords: groundwater; heavy metal(loid)s; ecological risk; health risk; Shule River Basin

Citation: WEN Xiaohu, LI Leiming, WU Jun, LU Jian, SHENG Danrui. 2023. Multiple assessments, source determination, and health risk apportionment of heavy metal(loid)s in the groundwater of the Shule River Basin in northwestern China. Journal of Arid Land, 15(11): 1355–1375. https://doi.org/10.1007/s40333-023-0111-7

*Corresponding author: LI Leiming (E-mail: lileiming@isl.ac.cn)
Received 2023-05-17; revised 2023-08-31; accepted 2023-09-08

1 Introduction

Heavy metal(loid)s pollution has attracted interest worldwide due to the toxicity of these elements and their ability to enter the food chain, resist degradation, and persist (Wu et al., 2016; Li et al., 2018; Cui et al., 2022; Huang et al., 2022). There are reports of significant annual heavy metal(loid)s discharge into waters worldwide (Gao et al., 2020; Jaskuła and Sojka, 2022). Heavy metal(loid)s have the capacity to concentrate in aquatic species after the elements enter waters. When the concentrations of heavy metal(loid)s are higher than what aquatic organisms can tolerate, they have disastrous effects on the organisms (Vatanpour et al., 2020; Adegbola et al., 2021). Heavy metal(loid)s pose a severe threat to humans since they can enter the body in large quantities through the food chain and have teratogenic and carcinogenic consequences (Mukherjee et al., 2020; Liu et al., 2022). The threats that heavy metal(loid)s pose to the environment and human health must be considered (Wei et al., 2022; Wu et al., 2022), together with assessments of pollution, water quality, and other factors.

Heavy metal(loid)s pollution in waters has been extensively characterized using the Nemerow pollution index (NP), heavy metal evaluation index (HEI), degree of contamination (DC), and heavy metal pollution index (HPI) (Mohan et al., 1996; Backman et al., 1997; Edet and Offiong, 2002; Saleem et al., 2019; Karunanidhi et al., 2022; Li et al., 2022). The ecological risk index (ERI) and water quality index (WQI) are well known as crucial tools for providing a comprehensive picture of the ecological hazards and water quality of groundwater, rivers, and lakes (Prabakaran et al., 2020; Ustaoğlu et al., 2020; de Carvalho et al., 2021). The origins of heavy metal(loid)s in waters are frequently identified using three multivariate statistical techniques, including principal component analysis (PCA), factor analysis (FA), and correlation analysis (Li et al., 2020a; Lu et al., 2022a, b). The source apportionment of heavy metal(loid)s in waters has recently been studied using receptor models, such as positive matrix factorization (PMF) model, absolute principal component scores-multiple linear regression (APCS-MLR) model, UNMIX, and chemical mass balance (CMB) (Chai et al., 2021; Lei et al., 2022; Proshad et al., 2022). Additionally, the health risk assessment model has been used to analyze the noncarcinogenic and carcinogenic dangers of heavy metal(loid)s found in waters (Liu et al., 2019; Sheng et al., 2021, 2022). Prior studies have given attention to the effects of pollution sources on the concentrations of heavy metal(loid)s in waters.

To prevent health issues and ensure effective control, it is helpful to quantify source-specific health risk partitioning of heavy metal(loid)s in waters. Nonetheless, the significant spatial heterogeneity of heavy metal(loid)s in waters caused by various contamination sources (anthropogenic and natural) makes the quantitative partitioning of source-specific health risk difficult. Parent material weathering and pedogenesis are regarded as the main natural sources of heavy metal(loid)s in waters. Anthropogenic sources include activities such as irrigation with sewage, metal smelting and mining, industrial activities, and the indiscriminate use of pesticides, fertilizers, livestock manures, or herbicides (Wu et al., 2021; Sheng et al., 2022). The distribution, prevalence, and toxicity of heavy metal(loid)s are significantly influenced by a variety of sources and should be highlighted (Wen et al., 2019; Guo et al., 2021). As a result, a source-specific health risk apportionment approach, which takes into account both source apportionment and health risk assessment, is needed. To safeguard human health, it is essential to comprehend the specific health problems that heavy metal(loid)s in water create at each source.

The Heihe River Basin, which is close to this study area, has high SO_4^{2-} concentrations in the river and shallow groundwater (Li et al., 2013; Xie et al., 2022). Current studies on the groundwater or freshwater in the Shule River Basin have prioritized water quantity, ecosystem service assessment, and water salinization and evolution (Guo et al., 2015; Zhou et al., 2021; Xie et al., 2022; Yue et al., 2022a, b). The causes of the Shule River Basin contamination and associated health issues have not yet been properly pinpointed. Therefore, it is important and necessary to evaluate the impact of heavy metal(loid)s from pollution sources on health risk. The main goals of this study were to (1) assess the pollution level of heavy metal(loid)s based on

various indices (including DC, HEI, HPI, and NP); (2) evaluate water quality and ecological risk using the WQI and ERI, respectively; (3) choose a method that is appropriate for allocating heavy metal(loid)s pollution sources by comparing PMF model and APCS-MLR model; and (4) determine the source-specific health risks of heavy metal(loid)s.

2 Materials and methods

2.1 Study area

The Shule River is an inland river located at the western end of the northwestern Hexi Corridor. It originates in the Qilian Mountains and flows through the Yumen-Tashi subbasin before dissipating in the lower Gobi desert (Xie et al., 2022). Groundwater and rivers provide significant water supplies for oases. Near Changma Town, Huahai Town, and Shuangta Town, the water is mostly used for agricultural irrigation (Guo et al., 2015; Xie et al., 2022). Due to the significant agricultural labor force that had become established in the region by 2020, the population reached 5.4×10^5. Additionally, more than 1.3×10^3 km^2 land was irrigated for cultivation during the same period (Gansu Provincial Water Resources Department, 2020). Consequently, the ecosystem of the Shule River Basin is highly vulnerable (Yue et al., 2022a, b). In addition, both the population and the intensity of resource use have dramatically expanded in recent years (Zhou et al., 2021).

The study area is located in the Shule River Basin (39°32′–41°53′N, 92°46′–98°26′E; Fig. 1). The Shule River Basin spans 4.13×10^4 km^2 in Gansu Province's northwest region. The Shule River starts from the Qilian Mountains, where meltwater is plentiful. The National Outline of Ecological Environment Conservation has identified the downstream section of the Shule River Basin as a significant region for soil and water conservation. The Shule River Basin is an area of irrigated farmland with a long history (Yue et al., 2022b). The middle and lower basin regions as well as those in the northern Mazong Mountains region with bare rock, sandy ground, and the Gobi desert are particularly sensitive to environmental changes (Qi et al., 2017).

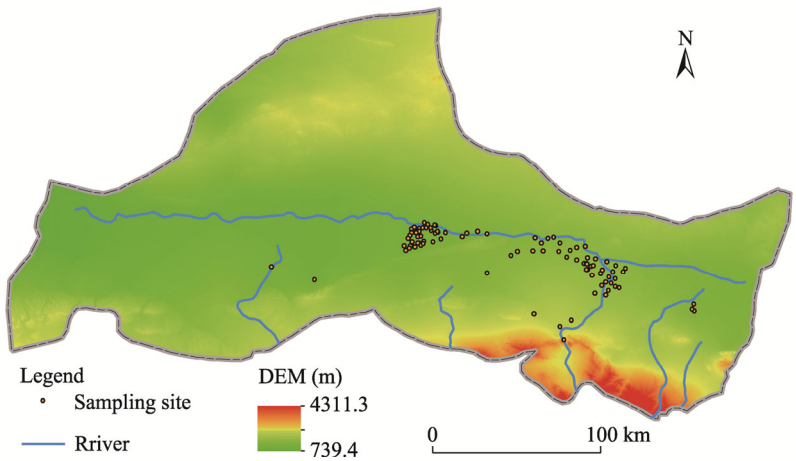

Fig. 1 Distribution of sampling sites. DEM, digital elevation model.

2.2 Sample collection and analysis

A total of 96 groundwater samples were collected from the Shule River Basin in August 2018. The temperature, dissolved oxygen content (DO), pH, total dissolved solids (TDS), and electrical conductivity (EC) of each groundwater sample were measured in situ using an Ultrameter II^{TM} 6P (Myron L Company, CA, USA).

The groundwater samples were stored in prewashed polypropylene bottles after collection and were transported to the laboratory. All samples were processed through 0.45 m membrane filters, acidified with nitric acid (pH<2), and then kept at 4°C before further examination. We used ion chromatography to investigate the concentration of several cations and anions (including Na^+,

Mg^{2+}, K^+, Ca^{2+}, Cl^-, NO_3^-, and SO_4^{2-}). The concentration of HCO_3^-/CO_3^{2-} was determined by a volumetric method. Heavy metal(loid)s, including manganese (Mn), aluminum (Al), cobalt (Co), ferrum (Fe), cuprum (Cu), nickel (Ni), arsenic (As), zinc (Zn), lead (Pb), and cadmium (Cd), were analyzed using an ELAN DRC II inductively coupled plasma mass spectrometer (PerkinElmer Ltd., MA, USA). Table S1 shows the detection and quantification limits for the heavy metal(loid)s in the groundwater samples. For quality control during this analysis, we used spiked blanks, spiked samples, and duplicate technique blanks. The tested substance's relative standard deviation (RSD) was less than 15.0%, which met the criteria of United States Environmental Protection Agency (RSD below 30.0%). The 10 heavy metal(loid)s measured in this study had average recovery rates ranging from 89.2% to 108.7%.

2.3 Pollution and assessment

DC, HEI, HPI, and NP were used to evaluate pollution levels in the groundwater (Mohan et al., 1996; Backman et al., 1997; Edet and Offiong, 2002; Saleem et al., 2019; Karunanidhi et al., 2022; Li et al., 2022). These indices were calculated by the following formulas:

$$\mathrm{DC} = \sum_{i=1}^{n}\left(\frac{C_i}{MAC_i} - 1\right), \tag{1}$$

$$\mathrm{HEI} = \sum_{i=1}^{n}\frac{C_i}{MAC_i}, \tag{2}$$

$$\mathrm{HPI} = \frac{\sum_{i=1}^{n}\left(\frac{1}{S_i}\times\frac{C_i}{S_i}\times 100\right)}{\sum_{i=1}^{n}\frac{k}{S_i}}, \tag{3}$$

$$\mathrm{NP} = \sqrt{\frac{\left(\frac{C_i}{S_i}\right)_{\mathrm{mean}}^2 + \left(\frac{C_i}{S_i}\right)_{\mathrm{max}}^2}{2}}, \tag{4}$$

where C_i is the analyzed concentration of heavy metal(loid)s in the groundwater samples (μg/L); S_i and MAC_i adopted the standards of the Chinese drinking water or World Health Organization (WHO) (Ministry of Health of the People's Republic of China, 2006; World Health Organization, 2011), respectively; n denotes the amount of heavy metal(loid)s; and k is a proportionality constant. The ranking criteria for DC, HEI, HPI, and NP are based on Sheng et al. (2022).

2.4 Water quality index (WQI) and ecological risk index (ERI)

2.4.1 WQI

The WQI is regarded as a useful tool for comprehensively understanding the water quality of groundwater, rivers, or lakes (Tiwari and Mishra, 1985; Xu et al., 2020). The WQI brings together a large number of water quality characteristics (physical-chemical parameters and heavy metal(loid)s) from a large amount of data (Ravindra et al., 2019; Ustaoğlu et al., 2020; de Carvalho et al., 2021). The WQI is calculated using the following formula:

$$\mathrm{WQI} = \sum\left[W_i \times \left(\frac{C_i}{S_i}\right)\right] \times 100, \tag{5}$$

where W_i is the relative weight. The W_i can be calculated using the following equation:

$$W_i = w_i / \sum w_i, \tag{6}$$

where w_i is the weight of each parameter, according to its relative effects on suitability for consumption and human health risks (Şener et al., 2017; Li et al., 2022); and Σw_i is the sum of w_i, and Σw_i is 47 in this study. The ranking standards of the WQI are based on Li et al. (2022).

2.4.2 ERI

Ecological risk analysis has often been performed to evaluate the potential effects of heavy metal(loid)s contamination on organisms. The ERI, which is often employed in the ecological risk evaluation of habitats in water, is generated using the following formula (Li et al., 2018; Qin et al., 2021; Karunanidhi et al., 2022):

$$\mathrm{ERI} = \sum_{i=1}^{n} T_i \times \frac{C_i}{S_i}, \tag{7}$$

where T_i is the biological toxicity factor of target heavy metal(loid)s. Hakanson (1980) showed the T_i of every heavy metal(loid). The classifications of the ERI are presented in Sheng et al. (2022).

2.5 Source apportionment analysis

Analysis of the sources of contaminants in water, soil, and air is frequently performed using PMF model. Environmental Protection Agency Positive Matrix Factorization 5.0 is often used to calculate the source apportionment of heavy metal(loid)s in groundwater or surface water. In multiple linear regressions, the concentrations of heavy metal(loid)s were used as the dependent variables, and in APCS-MLR model, the absolute principal component factor scores were used as the independent variables. The regression coefficient is used to calculate each pollutant source's contribution. SPSS 22.0 software was used to calculate APCS-MLR model. Sheng et al. (2022) provided an overview of the mathematical expression computation process used for PMF model and APCS-MLR model.

2.6 Source-specific health risk assessment

To assess the level of toxicity that heavy metal(loid)s produce in aquatic ecosystems, researchers frequently utilized hazard quotients in previous studies (Özgür et al., 2020; de Carvalho et al., 2021; Githaiga et al., 2021). The hazard index is employed to evaluate all potential noncarcinogenic risks brought on by various methods (USEPA, 2004; Wu et al., 2018). Only heavy metal(loid)s with carcinogenic slope factors are evaluated for carcinogenic risk (Özgür et al., 2020; Li et al., 2022). The health risk assessment model and APCS-MLR model were combined to calculate the source-specific health hazards for residential and recreational receptors (USEPA, 2011). Sheng et al. (2022) provided a summary of the mathematical statement and calculation process for health risk.

2.7 Data analysis

Spearman correlation was utilized to evaluate the correlations among heavy metal(loid)s from groundwater, surface water, soil, sediment, and so on (Li et al., 2020b, 2022; Lu et al., 2022a, b). PCA is a statistical technique adopted to quickly obtain information by converting a collection of initial connected variables into values of principal components, which are linearly uncorrelated variables (Li et al., 2020a). The objective of FA, which is closely related to PCA, is to produce a lower-dimensional linear structure that conveys the main message of the original data (Sheng et al., 2022). The comprehensive PCA and FA information is reported in Sheng et al. (2022).

3 Results and discussion

3.1 Concentrations of heavy metal(loid)s

Descriptive information on total dissolved solids (TDS), concentration of anions and cations, DO, pH, EC, and temperature of groundwater was shown in Table S1. TDS values varied significantly among the samples, with values ranging from 301.0 to 7009.0 mg/L. Excessive TDS led to reduced water clarity, hinders photosynthesis, and increases water temperature (Rahman and Gagnon, 2014). Moreover, TDS values for 49.0% of the sampling sites exceeded the WHO guideline value (1000.0 mg/L). The concentrations of anions were measured, and they were ranked in the order of

SO_4^{2-}>NO_3^->Cl^-. Approximately 61.5% of the sampling sites for SO_4^{2-} exceeded the limit of detection values, while 39.6% and 36.5% of the sampling sites for NO_3^- and Cl^- exceeded the limit of detection values, respectively. The cations results revealed that more than 38.5% of the sampling sites had Na^+, Mg^{2+}, K^+, and Ca^{2+} levels that were much higher than their standard reference values. The average value of DO was 7.4 mg/L and DO of groundwater ranged from 2.8 to 18.5 mg/L. The average pH was 8.0 with a range between 7.2 and 9.4, indicating that the groundwater was slightly alkaline. EC ranged from 446.0 to 7480.0 μS/cm, with an average value of 2025.0 μS/cm. Higher EC indicated greater water contamination (Florescu et al., 2011). It may be inferred from the physical-chemical parameter and anion and cation studies that the groundwater of the Shule River Basin was unsatisfactory with respect to TDS, concentrations of anions and cations, and EC values.

The concentrations of the 10 heavy metal(loid)s were shown in Table S1 and Figure 2. The mean concentrations of heavy metal(loid)s in groundwater decreased in the following order: Fe>Zn>Ni>Al>Cu>As>Mn>Co>Pb>Cd. The mean concentrations of these nine heavy metal(loid)s, namely, Zn, Ni, Al, Cu, As, Mn, Co, Pb, and Cd, were below the WHO and Chinese drinking standards for the corresponding metal(loid)s (Ministry of Health of the People's Republic of China, 2006; World Health Organization, 2011). For Fe, only 39.6% of the groundwater samples surpassed the threshold. The concentrations of Fe in the groundwater of this area indicated that Fe was the primary contaminant in the groundwater of the Shule River Basin. The human body needs the elements, including Fe, Zn, Cu, and Mn (Sheng et al., 2022). The spatial distributions of the target heavy metal(loid)s, such as Fe, Mn, Ni, Co, As, Cu, Pb, and Cd, were similar (Fig. S1). Al and Zn had their own spatial distribution characteristics. To fully understand the pollution status of heavy metal(loid)s in the groundwater of the Shule River Basin, we compared the concentrations of heavy metal(loid)s in this study area with those of other rivers or groundwaters in eastern China (Table S2). For instance, the concentration of Fe in this study area was much higher than that in the rivers or groundwaters of the Heihe River, Buh River, Yellow River, and Za'gya Zangbo River, northeastern Qinghai-Tibet Plateau, Yangtze River, Lancang River (Mekong River), Salween River (Nujiang River), Yarlung Zangbo River, Ganges River, Indus River, Chinese Loess Plateau, Tarim River Basin, and Zhangye Basin (Huang et al., 2009; Zheng et al., 2010; Xiao et al., 2014; Qu et al., 2015; Zhang et al., 2015; Qu et al., 2017; Qu et al., 2019; Xiao et al., 2019; Li et al., 2022; Sheng et al., 2022). Overall, different regions of eastern China had quite variable concentrations of heavy metal(loid)s in rivers. Given that many of heavy metal(loid)s can be extremely harmful even at low quantities in groundwater, it is essential to establish effective groundwater management methods to ensure safe groundwater supply.

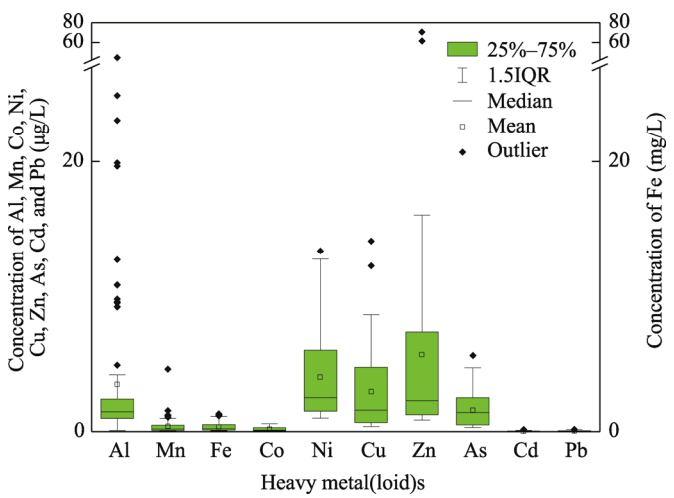

Fig. 2 Variation of heavy metal(loid)s in groundwater samples of the Shule River Basin. Al, aluminum; Mn, manganese; Fe, ferrum; Co, cobalt; Ni, nickel; Cu, cuprum; Zn, zinc; As, arsenic; Cd, cadmium; Pb, lead; IQR, interquartile range.

3.2 Pollution assessment

For regional environmental management, more knowledge on the overall contamination caused by the presence of heavy metal(loid)s in groundwater is needed. Four methods, including DC, HEI, HPI, and NP, were utilized to evaluate the degree of pollution caused by all target heavy metal(loid)s in groundwater (Fig. 3). The four index values at each sampling site had similar spatial distributions. However, the results showed that the hazard posed by all heavy metal(loid)s was minimal in the great majority of groundwater samples from the Shule River Basin.

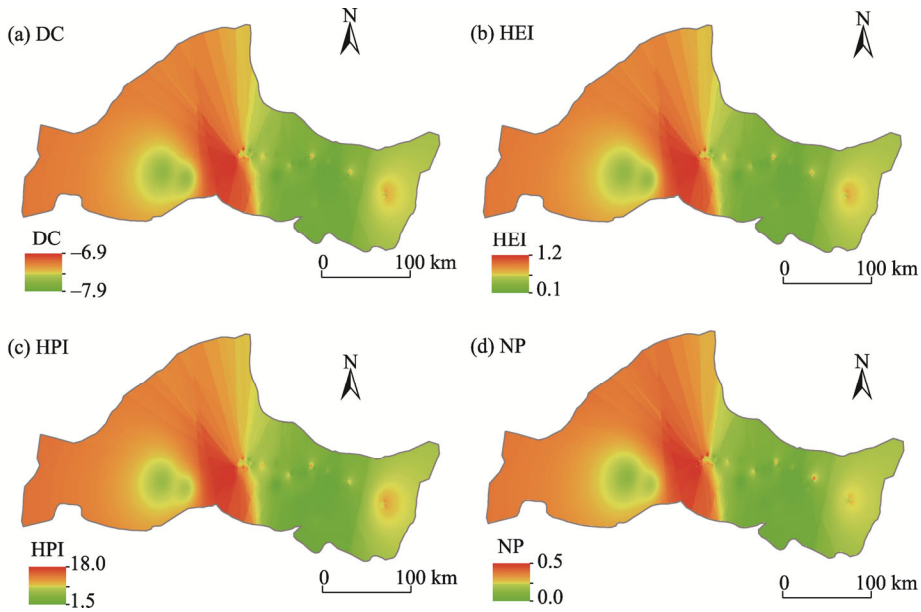

Fig. 3 Spatial distribution of degree of contamination (DC; a), heavy metal evaluation index (HEI; b), heavy metal pollution index (HPI; c), and Nemerow pollution index (NP; d) for groundwater in the Shule River Basin

DC and HEI were established by integrating the variables' maximum permitted concentrations (Fig. 3a and b). DC values ranged from –7.9 to –6.7, with a mean value of –7.6. HEI values ranged from 0.1 to 1.3, with a mean of 0.4. HEI for all samples was below the threshold of 10.0, according to the index data, suggesting a pollution-free state. The mean HPI value for heavy metal(loid)s in groundwater samples was 5.7, with values ranging from 1.4 to 19.2 (Fig. 3c). According to HPI rating standards, low and moderate pollution was present at 96.9% and 3.1% of the sampling sites, respectively (Qiao et al., 2020). Ni and As mainly accounted for moderate degrees of contamination as evaluated by HPI in only three sites. In numerous earlier studies, NP has been used to assess the total pollution from heavy metal(loid)s in water samples (Li et al., 2022). NP values consider the median and maximum concentrations of each heavy metal(loid) and can show the significance of major and severe contaminants (Karunanidhi et al., 2022; Mahmudul et al., 2022). The mean NP value for heavy metal(loid)s in groundwater samples was 0.2, with values ranging from 0.0 to 0.5 (Fig. 3d). According to NP rating standards (Li et al., 2018), all sampling sites showed low pollution levels.

3.3 Results of the ERI and WQI

The ERI values on the whole ranged from 0.7 to 9.4, with a mean of 2.8 (Fig. 4). All samples met the "low risk" ranking criteria set forth by the ERI (Karunanidhi et al., 2022). The findings revealed that none of the data from the water samples taken from the groundwater in the study area indicated that heavy metal(loid)s caused harm to the environment.

The groundwater quality of the Shule River Basin was further examined using the WQI (Fig. 4a). The determination of water quality was carried out using 14 different water parameters. The

four categories of water samples are excellent water quality, good water quality, poor water quality, and very poor water quality, with the first three being drinkable and the last two being unfit for consumption (Li et al., 2022). The WQI values of the groundwater in the Shule River Basin ranged from 9.7 to 248.0, with an average of 64.4. The groundwater in 58.3%, 12.5%, 27.1%, and 2.1% of the sampling sites had excellent water quality, good water quality, poor water quality, and very poor water quality, respectively. The water quality of the Shule River Basin was generally excellent. According to the geographic distribution of the WQI in groundwater, the good water quality samples with low WQI values were distributed in the eastern Shule River Basin, and the higher values were distributed in the western Shule River Basin. In the study area, evaporation is high, while precipitation is minimal. The western end of the Shule River Basin shows sites with erosion and desertification. The high concentrations of Fe, cations (Na^+, Mg^{2+}, K^+, and Ca^{2+}), and anions (Cl^-, NO_3^-, and SO_4^{2-}) in the groundwater of the Shule River Basin were associated with a high WQI. The findings indicated that the western groundwater resources were only appropriate for irrigation, while the eastern groundwater resources could be used for irrigation and consumption.

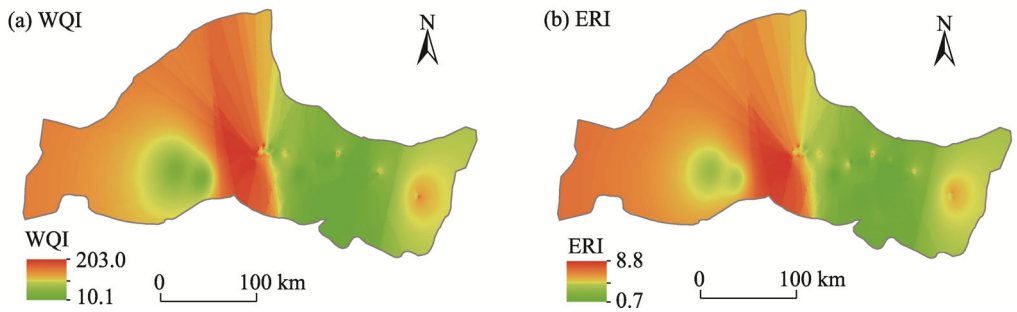

Fig. 4 Spatial distribution of water quality index (WQI; a) and ecological risk index (ERI; b) for groundwater in the Shule River Basin

3.4 Positive matrix factorization (PMF) model and absolute principal component scores-multiple linear regression (APCS-MLR) model comparisons

PMF model and APCS-MLR model were utilized to determine the sources of the heavy metal(loid)s in the groundwater (Table 1). The representative heavy metal(loid)s from a particular source were considered to be those heavy metal(loid)s with a high loading among the factors in groundwater. APCS-MLR model retrieved three components. The R^2 values for the 10 metal(loid)s in APCS-MLR model were more than 0.629, indicating effective fitting (Fig. 5). Factor 1 (human activities and the initial geological environment factor) was primarily responsible for Mn, Fe, Ni, Co, Cu, As, Cd, and Pb, with contributions of 56.1%, 88.6%, 88.2%, 89.0%, 90.0%, 93.3%, 75.9%, and 64.1%, respectively. Factor 2 (industrial activity factor) explained 94.0% of the concentration of Al. Factor 3 (agricultural practices factor; 84.2%) had the highest concentration of Zn, making Zn the dominant element in Factor 3.

We selected three PMF model components based on their smallest and steadiest Q values, similar to APCS-MLR model (Table 1). According to U.S. Environmental Protection Agency (USEPA) PMF model, Figure 6 displays the "factor figure-prints" of all target heavy metal(loid)s in groundwater, which represents a conceptual fraction of possible pollution contributions. Heavy metal(loid)s were classified as "strong" because they had a signal-to-nose ratio of 10, which ensured the plausibility of PMF model. The remaining heavy metal(loid)s had R^2 values greater than 0.765, with the exception of Al, Mn, and Zn. Factor 1 had the highest contribution from Cd, Mn, and Al, with values ranging from 43.1% to 62.2%, as shown in Figure 6 and Table 1. Factor 2 was dominated by Fe (70.4%), Co (65.0%), Ni (66.8%), Cu (48.9%), Zn (51.7%), and Pb (50.4%). As made a 56.0% contribution to Factor 3.

Table 1 Contribution of each factor derived from positive matrix factorization (PMF) model and absolute principal component scores-multiple linear regression (APCS-MLR) model

Heavy metal(loid)s	PMF model				APCS-MLR model			
	Factor 1 (%)	Factor 2 (%)	Factor 3 (%)	R^2	Factor 1 (%)	Factor 2 (%)	Factor 3 (%)	R^2
Al	62.2	0.1	37.7	0.005	2.0	94.0	4.0	0.899
Mn	43.1	31.2	25.7	0.418	56.1	33.6	15.3	0.629
Fe	16.4	70.4	13.1	1.000	88.6	1.8	9.6	0.944
Co	21.1	65.0	13.9	0.916	89.0	0.6	10.3	0.926
Ni	18.3	66.8	14.8	0.983	88.2	1.8	10.0	0.938
Cu	12.0	48.9	39.1	0.907	90.0	0.4	9.6	0.906
Zn	17.9	51.7	30.4	0.073	14.5	1.3	84.2	0.987
As	18.4	25.6	56.0	1.000	93.3	0.3	6.4	0.876
Cd	59.2	26.4	14.4	1.000	75.9	10.3	13.8	0.834
Pb	38.3	50.4	11.4	0.765	64.1	20.3	15.6	0.882

Note: Al, aluminum; Mn, manganese; Fe, ferrum; Co, cobalt; Ni, nickel; Cu, cuprum; Zn, zinc; As, arsenic; Cd, cadmium; Pb, lead. Factor 1 represents human activities and the initial geological environment factor, Factor 2 represents industrial activity factor, and Factor 3 represents agricultural practices factor.

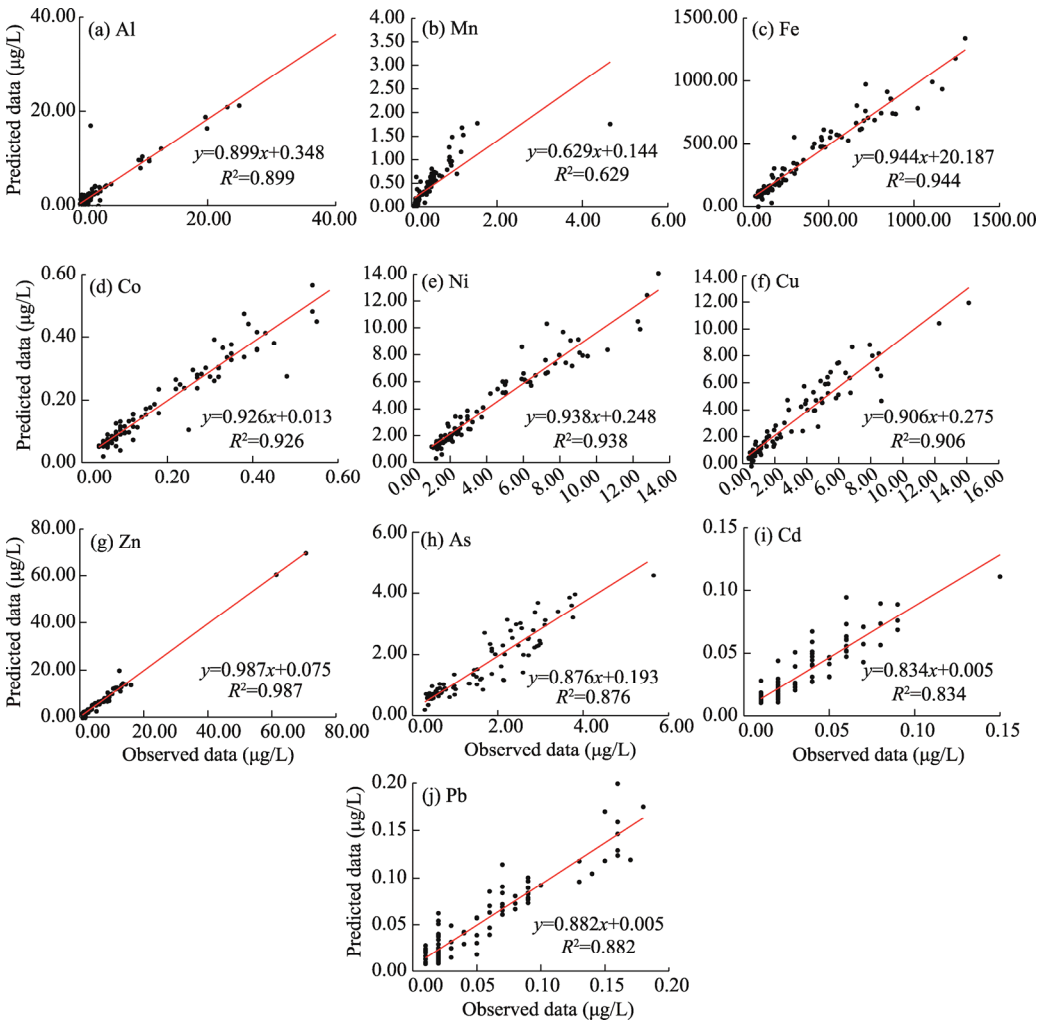

Fig. 5 Scatter plot of observed data and predicted data derived from absolute principal component scores-multiple linear regression (APCS-MLR) model. (a), Al; (b), Mn; (c), Fe; (d), Co; (e), Ni; (f), Cu; (g), Zn; (h), As; (i), Cd; (j), Pb.

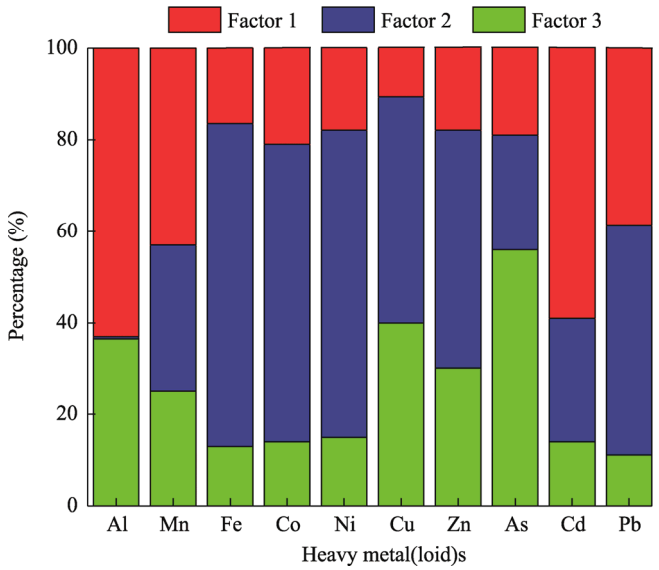

Fig. 6 Factor figure-prints of heavy metal(loid)s resulted from positive matrix factorization (PMF) model. Factor 1 represents human activities and the initial geological environment factor, Factor 2 represents industrial activity factor, and Factor 3 represents agricultural practices factor.

Both APCS-MLR model and PMF model correctly identified different types of pollution sources with three components for the two models. However, APCS-MLR model outperformed PMF model in terms of pollution source apportionment, as evidenced by the fact that its R^2 values were higher (Table 1). Additionally, a comparison of PMF model and APCS-MLR model predicted data versus observed data for most of the heavy metal(loid)s showed that APCS-MLR model had a superior fit (Fig. 5). APCS-MLR model may be more appropriate for the pollution source apportionment of heavy metal(loid)s in groundwater of this study area where complex contaminants coexist.

3.5 Source apportionment

It is essential to have a clear and in-depth understanding of the main sources of contaminants because the groundwater pollution sources in the study area are complex and variable. Figure 7 displays the correlation values for the 10 heavy metal(loid)s found in groundwater. Significant positive connections among heavy metal(loid)s were discovered in groundwater, with the

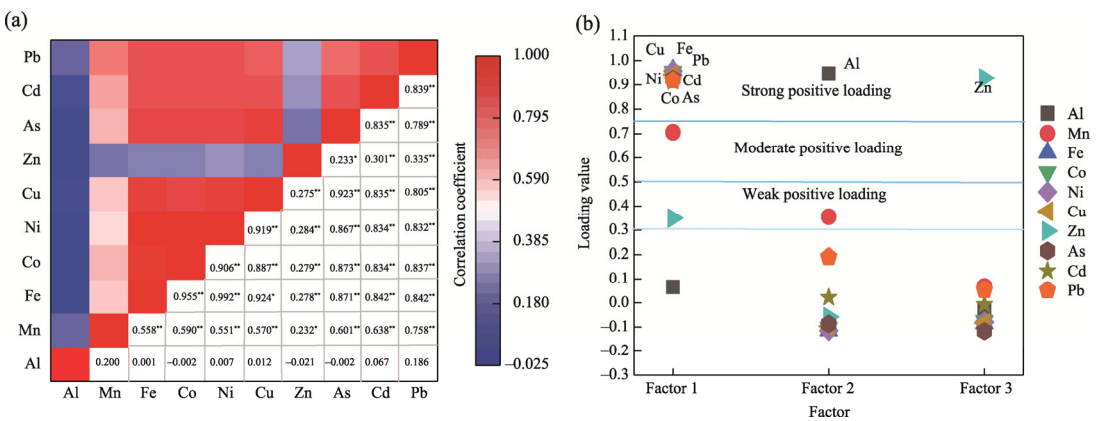

Fig. 7 Spearman correlation analysis among the groundwater heavy metal(loid)s (a) and component loading of the 10 measured heavy metal (loid)s on varimax rotated factors (b). ** indicates significant correlation at the level of 0.01, and * indicates significant correlation at the level of 0.05.

exception of Al and Zn, indicating that they might have comparable geochemical properties and origins. There was a substantial positive connection among Fe, Ni, Cu, As, Mn, Co, Pb, and Cd at the significance threshold of $P<0.01$.

Additionally, the factors influencing the distribution of heavy metal(loid)s in groundwater in the Shule River Basin were identified using PCA and FA. The Kaiser-Meyer-Olkin (KMO) value was 0.891, and the value of Bartlett's sphericity test was 1365.284 ($P<0.05$), indicating the validity of PCA and FA results. Figure 7b shows that the first three principal components account for 88.2% of the overall variation. Strong positive loadings were seen for Co (0.954), Fe (0.961), Cu (0.943), Ni (0.958), As (0.925), Pb (0.918), and Cd (0.913), while a moderate positive loading was seen for Mn (0.706). Factor 1 accounted for approximately 68.0% of the total variation. Factor 2 exhibited a substantial and positive loading of Al (0.946) and explained 11.1% of the overall variation. Factor 3 exhibited a substantial positive loading of Zn (0.928) and contributed 9.1% of the overall variance.

Furthermore, APCS-MLR model was used to quantify the sources of heavy metal(loid)s in groundwater and more clearly demonstrate the link. The results in Table 1 show that APCS-MLR model agreed with PCA and FA models. Fe, Mn, Ni, Co, As, Cu, Pb, and Cd had high loadings of 88.6%, 56.1%, 88.2%, 89.0%, 93.3%, 90.0%, 64.1%, and 75.9%, respectively. According to the examination of pollution indices, Fe was the main pollution source in the groundwater. Mn, Cu, Fe, Ni, Co, As, Pb, and Cd also displayed a discernible correlation based on Spearman correlation (Fig. 7a). Both the parent materials of the soil and agricultural practices such as irrigation and fertilization generated Fe and Cu contamination (Sheng et al., 2022). Most human activity in the basin is centered in the midstream and downstream reaches of the oasis region of the plain. It is a typical irrigation area with the most irrigated fields per person in Gansu Province and the Hexi region of China (Pan et al., 2021). Factor 1 corresponded to a large region that is primarily found in the east of the research area (Fig. 8). The dual influences of human activities and the initial geological environment are reflected in Factor 1, which is known as the "human activities and the initial geological environment factor". In APCS-MLR model, Factor 2 was weighted by Al (94.0%; Table 1). Factor 2 primarily dominated at three sites (Fig. 8). Factor 2 can be referred to as the "industrial activity factor" since it fits with the regional distribution pattern of other variables, and Al contamination was primarily affected by untreated industrial sewage. In APCS-MLR model, Factor 3 was represented by Zn and had a high loading of 84.2%. There were concentrated areas with high normalized concentrations of Factor 3 in the southeastern part of the study area where intensive agricultural practices enable substantial pesticide consumption (Fig. 8). Zn might be predominantly obtained from chemical substances applied during agricultural production according to earlier researches (Zhang et al., 2016; Sheng et al., 2022). These results suggested that human contributions might be the source of Zn in groundwater. More importantly, Zn in groundwater comes from oxidation and weathering processes in the crust of the Earth (Li et al., 2018). Factor 3 may be referred to as the "primary geological agricultural activity factor" due to the significant influence of agricultural productivity on the geological background.

The concentrations of the three variables that contributed to the buildup of heavy metal(loid)s in groundwater were mostly influenced by Factor 1 (65.9%; Fig. S2), followed by Factor 2 (16.4%). The contribution of Factor 3 was 17.8%. Sediments and the parent material of the Shule River Basin contributed to the accumulation of specific amounts of heavy metal(loid)s in groundwater, depending on the precedence of the factors. Heavy metal(loid)s associated with the makeup of the source material and the sediments are typically thought to be low-contamination elements. The concentrations of heavy metal(loid)s in the groundwater of the Shule River Basin were significantly influenced by natural variables, industrial processes, and agricultural nonpoint source pollution.

3.6 Source-specific health risk apportionment

APCS-MLR model provided the normalized heavy metal source contributions in water according to the acceptable daily intake. We used the 10 heavy metal(loid)s to evaluate the noncarcinogenic

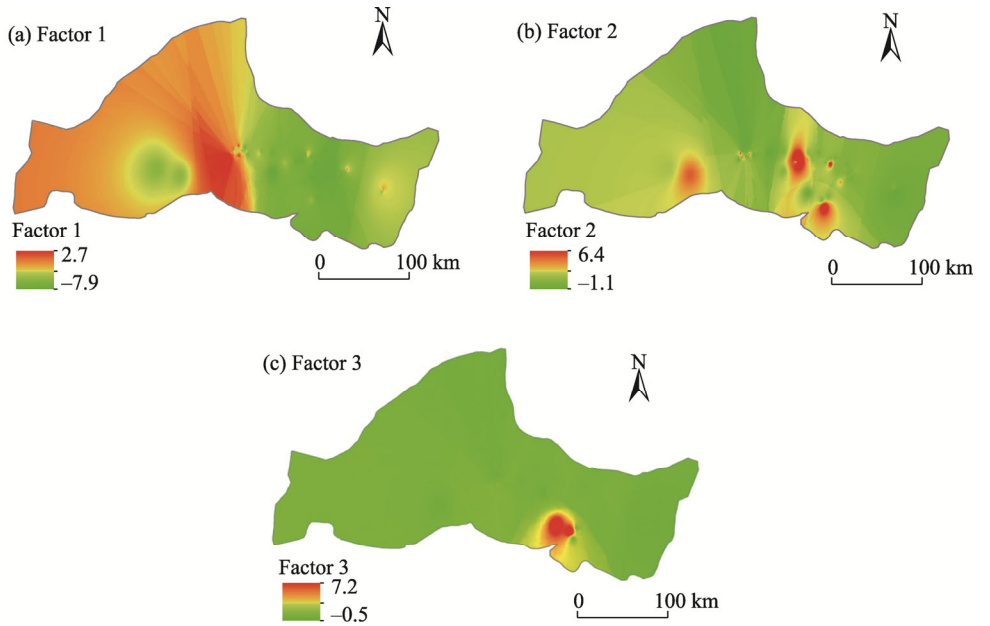

Fig. 8 Spatial distribution of normalized contribution for Factor 1 (a), Factor 2 (b), and Factor 3 (c)

and carcinogenic health hazards for four demographic categories, including residential children, residential adults, recreational children, and recreational adults, (Li et al., 2022) in the study area. The health risks originating from heavy metal(loid)s from various sources for all receptors are displayed in Figure 9 and Table 2.

Based on the contribution of each heavy metal(loid) acquired from APCS-MLR model, we calculated source-specific health hazards, including noncarcinogenic and carcinogenic hazards for residential children, residential adults, recreational children, and recreational adults (Table 2). It is

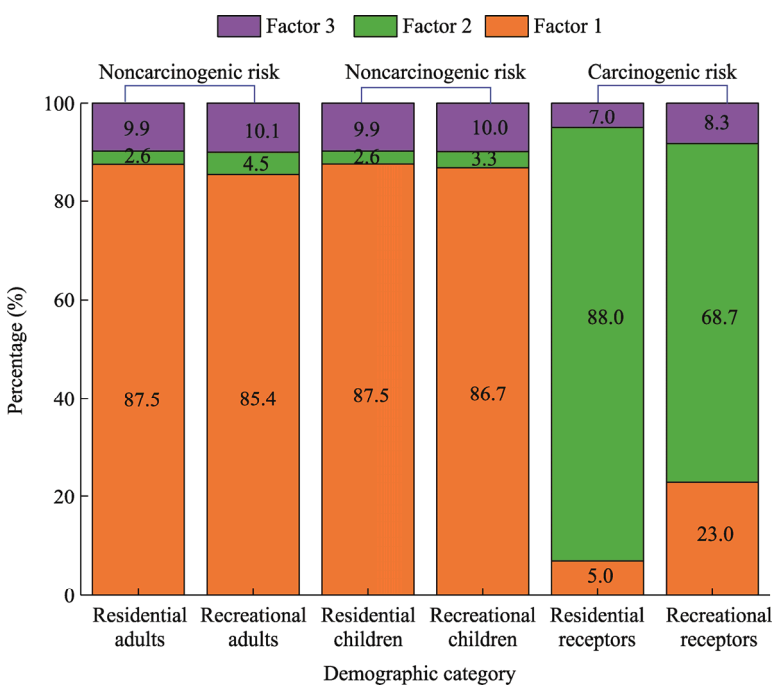

Fig. 9 Percentage of source-specific health risks from different source by APCS-MLR model for residential and recreational receptors

Table 2 Source-specific noncarcinogenic and carcinogenic risks of heavy metal(loid)s in groundwater of the Shule River Basin from different source for four demographic categories

	Factor 1	Factor 2	Factor 3	Total	Factor 1	Factor 2	Factor 3	Total
	Noncarcinogenic risk for residential adults				Noncarcinogenic risk for recreational adults			
Al	1.84×10^{-6}	8.63×10^{-5}	3.67×10^{-6}	9.18×10^{-5}	4.20×10^{-8}	1.97×10^{-6}	8.40×10^{-8}	2.10×10^{-6}
Mn	2.74×10^{-4}	1.64×10^{-4}	7.46×10^{-5}	4.88×10^{-4}	4.05×10^{-5}	2.43×10^{-5}	1.10×10^{-5}	7.22×10^{-5}
Fe	1.20×10^{-2}	2.44×10^{-4}	1.30×10^{-3}	1.35×10^{-2}	2.75×10^{-4}	5.58×10^{-6}	2.98×10^{-5}	3.10×10^{-4}
Co	1.43×10^{-3}	9.61×10^{-6}	1.65×10^{-4}	1.60×10^{-3}	2.76×10^{-5}	1.86×10^{-7}	3.19×10^{-6}	3.10×10^{-5}
Ni	4.64×10^{-3}	9.47×10^{-5}	5.26×10^{-4}	5.26×10^{-3}	8.42×10^{-5}	1.72×10^{-6}	9.55×10^{-6}	9.55×10^{-5}
Cu	1.75×10^{-3}	7.79×10^{-6}	1.87×10^{-4}	1.95×10^{-3}	4.01×10^{-5}	1.78×10^{-7}	4.28×10^{-6}	4.46×10^{-5}
Zn	7.32×10^{-5}	6.57×10^{-6}	4.25×10^{-4}	5.05×10^{-4}	1.51×10^{-6}	1.35×10^{-7}	8.76×10^{-6}	1.04×10^{-5}
As	1.30×10^{-2}	4.16×10^{-5}	8.88×10^{-4}	1.39×10^{-2}	2.97×10^{-4}	9.54×10^{-7}	2.04×10^{-5}	3.18×10^{-4}
Cd	1.33×10^{-3}	1.80×10^{-4}	2.41×10^{-4}	1.75×10^{-3}	3.04×10^{-5}	4.13×10^{-6}	5.53×10^{-6}	4.01×10^{-5}
Pb	6.15×10^{-4}	1.95×10^{-4}	1.50×10^{-4}	9.60×10^{-4}	1.08×10^{-5}	3.43×10^{-6}	2.64×10^{-6}	1.69×10^{-5}
THI	3.50×10^{-2}	1.03×10^{-3}	3.96×10^{-3}	4.00×10^{-2}	8.07×10^{-4}	4.25×10^{-5}	9.52×10^{-5}	9.41×10^{-4}
	Noncarcinogenic risk for residential children				Noncarcinogenic risk for recreational children			
Al	3.47×10^{-6}	1.63×10^{-4}	6.95×10^{-6}	1.74×10^{-4}	2.26×10^{-7}	1.06×10^{-5}	4.52×10^{-7}	1.13×10^{-5}
Mn	5.05×10^{-4}	3.02×10^{-4}	1.38×10^{-4}	9.00×10^{-4}	9.87×10^{-5}	5.91×10^{-5}	2.69×10^{-5}	1.76×10^{-4}
Fe	2.27×10^{-2}	4.60×10^{-4}	2.46×10^{-3}	2.56×10^{-2}	1.48×10^{-3}	3.01×10^{-5}	1.60×10^{-4}	1.67×10^{-3}
Co	2.70×10^{-3}	1.82×10^{-5}	3.12×10^{-4}	3.03×10^{-3}	1.66×10^{-4}	1.12×10^{-6}	1.93×10^{-5}	1.87×10^{-4}
Ni	8.78×10^{-3}	1.79×10^{-4}	9.95×10^{-4}	9.95×10^{-3}	5.32×10^{-4}	1.09×10^{-5}	6.03×10^{-5}	6.03×10^{-4}
Cu	3.31×10^{-3}	1.47×10^{-5}	3.53×10^{-4}	3.68×10^{-3}	2.16×10^{-4}	9.60×10^{-7}	2.30×10^{-5}	2.40×10^{-4}
Zn	1.39×10^{-4}	1.24×10^{-5}	8.04×10^{-4}	9.55×10^{-4}	8.71×10^{-6}	7.81×10^{-7}	5.06×10^{-5}	6.01×10^{-5}
As	2.45×10^{-2}	7.87×10^{-5}	1.68×10^{-3}	2.62×10^{-2}	1.60×10^{-3}	5.13×10^{-6}	1.09×10^{-4}	1.71×10^{-3}
Cd	2.51×10^{-3}	3.40×10^{-4}	4.56×10^{-4}	3.31×10^{-3}	1.64×10^{-4}	2.22×10^{-5}	2.98×10^{-5}	2.16×10^{-4}
Pb	1.16×10^{-3}	3.69×10^{-4}	2.83×10^{-4}	1.82×10^{-3}	6.99×10^{-5}	2.21×10^{-5}	1.70×10^{-5}	1.09×10^{-4}
THI	6.63×10^{-2}	1.94×10^{-3}	7.48×10^{-3}	7.56×10^{-2}	4.33×10^{-3}	1.63×10^{-4}	4.97×10^{-4}	4.99×10^{-3}
	Carcinogenic risk for residential receptors				Carcinogenic risk for recreational receptors			
As	6.67×10^{-7}	3.13×10^{-5}	1.33×10^{-6}	3.33×10^{-5}	2.39×10^{-8}	1.12×10^{-6}	4.77×10^{-8}	1.19×10^{-6}
Cd	1.93×10^{-6}	1.15×10^{-6}	5.25×10^{-7}	3.43×10^{-6}	4.37×10^{-7}	2.62×10^{-7}	1.19×10^{-7}	7.79×10^{-7}
TCR	2.59×10^{-6}	3.25×10^{-5}	1.86×10^{-6}	3.70×10^{-5}	4.61×10^{-7}	1.38×10^{-6}	1.67×10^{-7}	2.01×10^{-6}

Note: THI, total hazard index; TCR, total carcinogenic risk.

clear that the health hazards for different sources differed greatly. In the study area, there was no noncarcinogenic risk for any of the four demographic categories. The total hazard index values of all target heavy metal(loid)s for noncarcinogenic risk were 7.56×10^{-2}, 4.00×10^{-2}, 4.99×10^{-3}, and 9.41×10^{-4} for residential children, residential adults, recreational children, and recreational adults, respectively. Children had the largest susceptibility to noncarcinogenic risk, followed by adults, which could be due to differences in ingestion rates, individual physiological difference, and hand-to-mouth behavior (Cai et al., 2019; Sheng et al., 2021). Similar conclusions have been derived in previous studies (Saha et al., 2017; Rajasekhar et al., 2020; Josiah et al., 2022; Krati et al., 2022). There was modest carcinogenic risk to all receptors, as indicated by the total carcinogenic risk values for residential receptors (3.70×10^{-5}) and recreational receptors (2.01×10^{-6}), which fell between 1.00×10^{-3} and 1.00×10^{-1}. The spatial distributions of the hazard index and carcinogenic risk were similar (Fig. S3). According to past investigations, residential receptors showed a clearly greater total carcinogenic risk than recreational receptors (Xiao et al., 2019; Li et al., 2022).

For residential children, residential adults, recreational children, and recreational adults in the Shule River Basin, the noncarcinogenic risk from the three sources exhibited virtually the same trend (Fig. 9). The noncarcinogenic risk contributions from the three source factors varied across all receptors. In terms of noncarcinogenic risk that each source posed, the three top factors were determined to be Factor 1, Factor 3, and Factor 2. Natural sources (residential children: 87.6%; residential adults: 87.5%; recreational children: 86.8%; and recreational adults: 85.4%) made the largest contribution. Therefore, the contribution of inputs should be neglected.

The Factor 3 came in second, followed by Factor 1, and Factor 2 was the source that contributed the most to the carcinogenic risk of the three sources. This indicates that human activities were mostly responsible for carcinogenic risk, and the contributions of Factor 2 to carcinogenic risk (residential receptors: 88.0%; and recreational receptors: 68.7%) were greater than the total contributions of the other two sources of heavy metal(loid)s (Fig. 9). Therefore, it is important to consider the contributions of inputs.

4 Conclusions

Source-specific health risk apportionment is of great significance for preventing and controlling potential groundwater heavy metal(loid)s pollution. In this study, the contamination characteristics, possible pollution sources, and source-specific health risks of heavy metal(loid)s in groundwater were analyzed for the Shule River Basin, Northwest China. The findings revealed that Fe had notable accumulation in groundwater, although DC, HEI, HPI, and NP indicated that the groundwater pollution levels were relatively low. The groundwater of the study area presented little ecological concern. However, only 58.3% of the groundwater samples were classified as good water quality. The factor corresponding to human activities and the initial geological environment was the most significant contributing factor to noncarcinogenic risk, while the industrial activity factor was the most significant contributor to carcinogenic risk, according to an evaluation of the health risks from heavy metal(loid)s in groundwater associated with the outcomes of APCS-MLR model. Both the carcinogenic and noncarcinogenic hazards for all types of receptors were similar in terms of the relative contributions of various sources. The leaching enrichment factor (65.9%) was the major source of noncarcinogenic risk, and the proportions for residential children, residential adults, recreational children, and recreational adults were 87.6%, 87.5%, 86.8%, and 85.4%, respectively. The industrial activity factor (16.4%) was the major source of carcinogenic risk, and the proportions for residential receptors and recreational receptors were 88.0% and 68.7%, respectively. There are no obvious noncarcinogenic concerns for any type of receptor and no obvious carcinogenic concerns in groundwater. The results signify that the risks due to heavy metal(loid)s in groundwater are likely to be negligible.

Conflict of interest

The authors declare that they have no known competing financial interests or personal relationships that could have appeared to influence the work reported in this paper.

Acknowledgements

This work was supported by the Kunlun Talent Action Plan of Qinghai Province (E140 WX42), National Natural Science Foundation of China (52179026), and Strategy for Water Resource Security in Yellow River Sources. The authors thank the editors and anonymous reviewers for their comments, which improved the manuscript.

Author contributions

Conceptualization: LI Leiming; Data curation: WEN Xiaohu; Methodology: WU Jun; Investigation: WEN Xiaohu; Formal analysis: WEN Xiaohu; Writing - original draft preparation: WEN Xiaohu; Writing - review and editing: WU Jun; Funding acquisition: LI Leiming; Resources: WEN Xiaohu; Supervision: LU Jian; Project administration: WEN Xiaohu; Software: SHENG Danrui; Validation: SHENG Danrui; Visualization: LI Leiming.

References

Adegbola I P, Aborisade B A, Adetutu A. 2021. Health risk assessment and heavy metal accumulation in fish species (*Clarias gariepinus* and *Sarotherodon melanotheron*) from industrially polluted Ogun and Eleyele Rivers, Nigeria. Toxicology Reports, 8: 1445–1460.

Backman B, Bodiš D, Lahermo P, et al. 1998. Application of a groundwater contamination index in Finland and Slovakia. Environmental Geology, 36: 55–64.

Cai L M, Wang Q S, Wen H H, et al. 2019. Heavy metals in agricultural soils from a typical township in Guangdong Province, China: Occurrences and spatial distribution. Ecotoxicological and Environmental Safety, 168: 184–191.

Canpolat Ö, Varol M, Okan Ö Ö, et al. 2020. A comparison of trace element concentrations in surface and deep water of the Keban Dam Lake (Turkey) and associated health risk assessment. Environment Research, 190: 110012, doi: 10.1016/j.envres.2020.110012.

Chai L, Wang Y H, Wang X, et al. 2021. Pollution characteristics, spatial distributions, and source apportionment of heavy metals in cultivated soil in Lanzhou, China. Ecological Indicators, 125: 107507, doi: 10.1016/j.ecolind.2021.107507.

Chen J W, Zhang H, Xue J Z, et al. 2022. Study on spatial distribution, potential sources and ecological risk of heavy metals in the surface water and sediments at Shanghai Port, China. Marine Pollution Bulletin, 181: 113923, doi: 10.1016/j.marpolbul.2022.113923

Cui L, Li J, Gao X Y, et al. 2022. Human health ambient water quality criteria for 13 heavy metals and health risk assessment in Taihu Lake. Frontiers of Environmental Science & Engineering, 16(4): 41, doi: 10.1007/s11783-021-1475-6.

de Carvalho V S, dos Santos I F, Almeida L C, et al. 2021. Spatio-temporal assessment, sources and health risks of water pollutants at trace levels in public supply river using multivariate statistical techniques. Chemosphere, 282: 130942, doi: 10.1016/j.chemosphere.2021.130942.

Edet A E, Offiong O E. 2002. Evaluation of water quality pollution indices for heavy metal contamination monitoring. A study case from Akpabuyo-Odukpani area, Lower Cross River Basin (southeastern Nigeria). GeoJournal, 57: 295–304.

Florescu D, Ionete R E, Sandru C, et al. 2011. The influence of pollution monitoring parameters in characterizing the surface water quality from Romania southern area. Romanian Journal of Physics, 56(7–8): 1001–1010.

Gansu Provincial Water Resources Department. 2020. Water Resources Bulletin of Gansu. [2023-05-10]. http://slt.gansu.gov.cn/lt/c106726/c106732/c106773/c106775/202110/1853946/files/d7c09d4d6a714a83ad058afddf9a492c.pdf.

Gao X Y, Wang X N, Li J, et al. 2020. Aquatic life criteria derivation and ecological risk assessment of DEET in China. Ecotoxicological and Environmental Safety, 188: 109881, doi: 10.1016/j.ecoenv.2019.109881.

Githaiga K B, Njuguna S M, Gituru R W, et al. 2021. Water quality assessment, multivariate analysis and human health risks of heavy metals in eight major lakes in Kenya. Journal of Environmental Management, 297: 113410, doi: 10.1016/j.jenvman.2021.113410.

Guo G H, Wang Y T, Zhang D G, et al. 2021. Source-specific ecological and health risks of potentially toxic elements in agricultural soils in Southern Yunnan Province and associated uncertainty analysis. Journal of Hazardous Materials, 417: 126144, doi: 10.1016/j.jhazmat.2021.126144.

Guo X Y, Feng Q, Liu W, et al. 2015. Stable isotopic and geochemical identification of groundwater evolution and recharge sources in the arid Shule River Basin of Northwestern China. Hydrological Processes, 29(22): 4703–4718.

Hakanson L, Håkanson L, Hakansonn L, 1980. An ecological risk index for aquatic pollution control: a sediment ecological approach. Water Research, 14: 975–1001.

Hasan M, Rahman M, al Ahmed A, et al. 2022. Heavy metal pollution and ecological risk assessment in the surface water from a marine protected area, Swatch of No Ground, north-western part of the Bay of Bengal. Regional Studies in Marine Science, 52: 102278, doi: 10.1016/j.rsma.2022.102278.

Huang X, Sillanpää M, Gjessing E T, et al. 2009. Water quality in the Tibetan Plateau: major ions and trace elements in the headwaters of four major Asian rivers. Science of the Total Environment, 407(24): 6242–6254.

Huang X G, Chen L H, Ma Z Q, et al. 2022. Cadmium removal mechanistic comparison of three Fe-based nanomaterials: Water-chemistry and roles of Fe dissolution. Frontiers of Environmental Science & Engineering, 16(12): 15–29.

Jabbo J N, Isa N M, Aris A Z, et al. 2022. Geochemometric approach to groundwater quality and health risk assessment of heavy metals of Yankari Game Reserve and its environs, Northeast Nigeria. Journal of Cleaner Production, 330: 129916, doi: 10.1016/j.jclepro.2021.129916.

Jaskuła J, Sojka M. 2022. Assessment of spatial distribution of sediment contamination with heavy metals in the two biggest rivers in Poland. CATENA, 211: 105959, doi: 10.1016/j.catena.2021.105959.

Karunanidhi D, Aravinthasamy P, Subramani T, et al. 2022. Provincial and seasonal influences on heavy metals in the Noyyal River of South India and their human health hazards. Environmental Research, 204: 111998, doi: 10.1016/j.envres.2021.111998.

Lei M, Li K, Guo G H, et al. 2022. Source-specific health risks apportionment of soil potential toxicity elements combining multiple receptor models with Monte Carlo simulation. Science of the Total Environment, 817: 152899, doi: 10.1016/j.scitotenv.2021.152899.

Li B, Chen Y, Chen Z, et al. 2013. Variations of temperature and precipitation of snowmelt period and its effect on runoff in the mountainous areas of Northwest China. Journal of Geographical Sciences, 23(1): 17–30.

Li L M, Wu J, Lu J, et al. 2018. Distribution, pollution, bioaccumulation, and ecological risks of trace elements in soils of the northeastern Qinghai-Tibet Plateau. Ecotoxicological and Environmental Safety, 166: 345–353.

Li L M, Wu J, Lu J, et al. 2020a. Speciation, risks and isotope-based source apportionment of trace elements in soils of the northeastern Qinghai-Tibet Plateau. Geochemistry: Exploration Environment Analysis, 20: 315–322.

Li L M, Wu J, Lu J, et al. 2020b. Trace elements in Gobi soils of the northeastern Qinghai-Tibet Plateau. Chemistry and Ecology, 36(10): 967–981.

Li L M, Wu J, Lu J, et al. 2022. Water quality evaluation and ecological-health risk assessment on trace elements in surface water of the northeastern Qinghai-Tibet Plateau. Ecotoxicological and Environmental Safety, 241: 10, doi: 10.1016/j.ecoenv.2022.113775.

Liu K H, Guan X J, Li C M, et al. 2022. Global perspectives and future research directions for the phytoremediation of heavy metal-contaminated soil: A knowledge mapping analysis from 2001 to 2020. Frontiers of Environmental Science & Engineering, 16(6): 73, doi: 10.1007/s11783-021-1507-2.

Liu L L, Tang Z, Kong M, et al. 2019. Tracing the potential pollution sources of the coastal water in Hong Kong with statistical models combining APCS-MLR. Journal of Environmental Management, 245(1): 143–150.

Lu J, Wu J, Wang J H. 2022a. Metagenomic analysis on resistance genes in water and microplastics from a mariculture system. Frontiers of Environmental Science & Engineering, 16(1): 4, doi: 10.1007/s11783-021-1438-y.

Lu J, Zhang Y X, Wu J, et al. 2022b. Intervention of antimicrobial peptide usage on antimicrobial resistance in aquaculture. Journal of Hazardous Materials, 427: 128154, doi: 10.1016/j.jhazmat.2021.128154.

Ministry of Health of the People's Republic of China. 2006. Standards for Drinking Water Quality (GB5749-2006). [2023-05-10]. https://std.samr.gov.cn/gb/search/gbDetailed?id=71F772D7FC82D3A7E05397BE0A0AB82A.

Mohan S V, Nithila P, Reddy S J. 1996. Estimation of heavy metal in drinking water and development of heavy metal pollution index. Journal of Environment Science, 31(2): 283–289.

Mukherjee I, Singh U K, Singh R P, et al. 2020. Characterization of heavy metal pollution in an anthropogenically and geologically influenced semi-arid region of east India and assessment of ecological and human health risks. Science of the Total Environment, 705: 135801, doi: 10.1016/j.scitotenv.2019.135801.

Pan N H, Guan Q Y, Wang Q Z, et al. 2021. Spatial differentiation and driving mechanisms in ecosystem service value of arid region: A case study in the middle and lower reaches of Shule River Basin, NW China. Journal of Cleaner Production, 319: 128718, doi: 10.1016/j.jclepro.2021.128718.

Prabakaran K, Eswaramoorthi S, Nagarajan R, et al. 2020. Geochemical behaviour and risk assessment of trace elements in a tropical river, Northwest Borneo. Chemosphere, 252: 126430, doi: 10.1016/j.chemosphere.2020.126430.

Proshad R, Uddin M, Idris A M, et al. 2022. Receptor model-oriented sources and risks evaluation of metals in sediments of an industrial affected riverine system in Bangladesh. Science of the Total Environment, 838(1): 156029, doi: 10.1016/j.scitotenv.2022.156029.

Qiao J B, Zhu Y J, Jia X X, et al. 2020. Distributions of arsenic and other heavy metals, and health risk assessments for groundwater in the Guanzhong Plain region of China. Environmental Research, 181: 108957, doi: 10.1016/j.envres.2019.108957.

Qi J H, Niu S W, Zhao Y F, et al. 2017. Responses of vegetation growth to climatic factors in Shule River Basin in Northwest China: A panel analysis. Sustainability, 9(3): 368, doi: 10.3390/su9030368.

Qin W J, Han D M, Song X F, et al. 2021. Sources and migration of heavy metals in a karst water system under the threats of an abandoned Pb-Zn mine, Southwest China. Environmental Pollution, 277: 116774, doi: 10.1016/j.envpol.2021.116774.

Qu B, Sillanpää M, Zhang Y L, et al. 2015. Water chemistry of the headwaters of the Yangtze River. Environmental Earth Sciences, 74(8): 6443–6458.

Qu B, Zhang Y L, Kang S C, et al. 2017. Water chemistry of the southern Tibetan Plateau: an assessment of the Yarlung Tsangpo river basin. Environmental Earth Sciences, 76(2): 74, doi: 10.1007/s12665-017-6393-3.

Qu B, Zhang Y L, Kang S C, et al. 2019. Water quality in the Tibetan Plateau: Major ions and trace elements in rivers of the "Water Tower of Asia". Science of the Total Environment, 649: 571–581.

Rahman M S, Gagnon G A. 2014. Bench-scale evaluation of drinking water treatment parameters on iron particles and water quality. Water Research, 48: 137–147.

Rajasekhar B, Nambi I M, Govindarajan S K. 2020. Human health risk assessment for exposure to BTEXN in an urban aquifer using deterministic and probabilistic methods: A case study of Chennai City, India. Environmental Pollution, 265(Part B): 114814, doi: 10.1016/j.envpol.2020.114814.

Ravindra K, Thind P S, Mor S, et al. 2019. Evaluation of groundwater contamination in Chandigarh: Source identification and health risk assessment. Environmental Pollution, 255: 113062, doi: 10.1016/j.envpol.2019.113062.

Saha N, Rahman M S, Ahmed M B, et al. 2017. Industrial metal pollution in water and probabilistic assessment of human health risk. Journal of Environmental Management, 185: 70–78.

Saleem M, Iqbal J, Shah M H. 2019. Seasonal variations, risk assessment and multivariate analysis of trace metals in the freshwater reservoirs of Pakistan. Chemosphere, 216: 715–724.

Şener Ş, Şener E, Davraz A. 2017. Evaluation of water quality using water quality index (WQI) method and GIS in Aksu River (SW-Turkey). Science of the Total Environment, 584–585: 131–144.

Sharma K, Raju N J, Neelratan S, et al. 2022. Heavy metal pollution in groundwater of urban Delhi environs: Pollution indices and health risk assessment. Urban Climate, 45: 101233, doi: 10.1016/j.uclim.2022.101233.

Sheng D R, Wen X H, Wu J, et al. 2021. Comprehensive probabilistic health risk assessment for exposure to arsenic and cadmium in groundwater. Environmental Management, 67(4): 779–792.

Sheng D, Meng X H, Wen X H, et al. 2022. Contamination characteristics, source identification, and source-specific health risks of heavy metals in groundwater of an arid oasis region in Northwest China. Science of the Total Environment, 841: 156733, doi: 10.1016/j.scitotenv.2022.156733.

Tiwari T N, Mishra M. 1985. A preliminary assignment of water quality index of major Indian rivers. Indian Journal of Environmental Protection, 5(4): 276–279.

USEPA. 2004. Risk Assessment Guidance for Superfund Volume I. Human Health Evaluation Manual (Part E, Supplemental Guidance for Dermal Risk Assessment). [2023-05-02]. https://cfpub.epa.gov/si/si_public_record_report.cfm?Lab=OSRTI&dirEntryId=82966.

USEPA. 2011. Exposure Factors Handbook 2011 Edition (Final Report). [2023-05-02]. https://cfpub.epa.gov/ncea/risk/recordisplay.cfm?deid=236252.

Ustaoğlu F, Tepe Y, Tas B. 2020. Assessment of stream quality and health risk in a subtropical Turkey river system: A combined approach using statistical analysis and water quality index. Ecological Indicators, 113: 105815, doi: 10.1016/j.ecolind.2019.105815.

Vatanpour N, Feizy J, Talouki H H, et al. 2020. The high levels of heavy metal accumulation in cultivated rice from the Tajan river basin: Health and ecological risk assessment. Chemosphere, 245: 125639, doi: 10.1016/j.chemosphere.2019.125639.

Wei Z S, Tang M R, Huang Z S, et al. 2022. Mercury removal from flue gas using nitrate as an electron acceptor in a membrane biofilm reactor. Frontiers of Environmental Science & Engineering, 16(2): 20, doi: 10.1007/s11783-021-1454-y.

Wen X H, Lu J, Wu J, et al. 2019. Influence of coastal groundwater salinization on the distribution and risks of heavy metals. Science of the Total Environment, 652: 267–277.

World Health Organization. 2011. Guidelines for Drinking-water Quality. [2023-05-02]. https://www.who.int/publications/i/item/9789240045064.

Wu H H, Xu C B, Wang J H, et al. 2021. Health risk assessment based on source identification of heavy metals: A case study of Beiyun River, China. Ecotoxicological and Environmental Safety, 213: 112046, doi: 10.1016/j.ecoenv.2021.112046.

Wu J, Duan D P, Lu J, et al. 2016. Inorganic pollution around the Qinghai-Tibet Plateau: An overview of the current observations. Science of the Total Environment, 550: 628–636.

Wu J, Lu J, Li L M, et al. 2018. Pollution, ecological-health risks, and sources of heavy metals in soil of the northeastern Qinghai-Tibet Plateau. Chemosphere, 201: 234–242.

Wu Y M, Leng Z R, Li J, et al. 2022. Sulfur mediated heavy metal biogeochemical cycles in coastal wetlands: From sediments, rhizosphere to vegetation. Frontiers of Environmental Science & Engineering, 16(8): 102, doi: 10.1007/s11783-022-1523-x.

Xiao J, Jin Z D, Wang J. 2014. Geochemistry of trace elements and water quality assessment of natural water within the Tarim River Basin in the extreme arid region, NW China. Journal of Geochemical Exploration, 136: 118–126.

Xiao J, Wang L Q, Deng L, et al. 2019. Characteristics, sources, water quality and health risk assessment of trace elements in river water and well water in the Chinese Loess Plateau. Science of the Total Environment, 650(2): 2004–2012.

Xu S, Lang Y C, Zhong J, et al. 2020. Coupled controls of climate, lithology and land use on dissolved trace elements in a karst river system. Journal of Hydrology, 591: 125328, doi: 10.1016/j.jhydrol.2020.125328.

Yu H, Lin M L, Peng W H, et al. 2022. Seasonal changes of heavy metals and health risk assessment based on Monte Carlo simulation in alternate water sources of the Xinbian River in Suzhou City, Huaibei Plain, China. Ecotoxicological and Environmental Safety, 236: 113445, doi: 10.1016/j.ecoenv.2022.113445.

Yue D X, Zhou Y Y, Guo J J, et al. 2022a. Relationship between net primary productivity and soil water content in the Shule River Basin. CATENA, 105770: 208, doi: 10.1016/j.catena.2021.105770.

Yue D X, Zhou Y Y, Guo J J, et al. 2022b. Ecosystem service evaluation and optimisation in the Shule River Basin, China. CATENA, 215: 106320, doi: 10.1016/j.catena.2022.106320.

Zhang G L, Bai J H, Zhao Q Q, et al. 2016. Heavy metals in wetland soils along a wetland-forming chronosequence in the yellow river delta of China: Levels, sources and toxic risks. Ecological Indicators, 69: 331–339.

Zhang Y L, Sillanpää M, Li C L, et al. 2015. River water quality across the Himalayan regions: elemental concentrations in headwaters of Yarlung Tsangbo, Indus and Ganges River. Environmental Earth Sciences, 73(8): 4151–4163.

Zheng W, Kang S C, Feng X B, et al. 2010. Mercury speciation and spatial distribution in surface waters of the Yarlung Zangbo River, Tibet. Chinese Science Bulletin, 55(24): 2697–2703.

Appendix

Table S1 Statistical summary of TDS, DO, pH, EC, temperature, and the concentrations of heavy metal(loid)s, anions, and cations of groundwater samples

Parameter	Minimum	Maximum	Mean	SD	CV (%)	Permissible value[#]	Percentage of SER (%)
Al (μg/L)	0.1	44.6	3.5	6.3	182.0	200.0	0.0
Mn (μg/L)	0.1	4.7	0.4	0.6	140.0	100.0	0.0
Fe (μg/L)	70.9	1300.0	358.0	306.0	85.7	300.0	39.6
Co (μg/L)	0.0	0.6	0.2	0.1	79.1	50.0	0.0
Ni (μg/L)	1.0	13.4	4.0	3.2	79.1	20.0	0.0
Cu (μg/L)	0.4	14.1	2.9	2.9	97.0	1000.0	0.0
Zn (μg/L)	0.9	70.7	5.7	9.8	170.0	1000.0	0.0
As (μg/L)	0.3	5.7	1.6	1.2	74.5	10.0	0.0
Cd (μg/L)	0.0	0.2	0.0	0.0	76.3	5.0	0.0
Pb (μg/L)	0.0	0.2	0.1	0.1	91.1	10.0	0.0
TDS (mg/L)	301.0	7009.0	1731.0	1484.0	85.7	1000.0	49.0
Na^+ (mg/L)	20.0	1358.0	243.0	244.0	100.0	200.0	38.5
Mg^{2+} (mg/L)	21.6	532.0	163.0	139.0	84.9	50.0	80.2
K^+ (mg/L)	3.0	49.9	13.5	11.8	87.2	10.0	42.7
Ca^{2+} (mg/L)	30.6	382.0	102.0	76.2	74.9	75.0	44.8
Cl^- (mg/L)	19.5	1155.0	262.0	263.0	101.0	250.0	36.5
NO_3^- (mg/L)	2.1	89.1	19.8	19.1	96.6	20.0	39.6
SO_4^{2-} (mg/L)	76.0	3522.0	749.0	757.0	101.0	250.0	61.5
HCO_3^-/CO_3^{2-} (mg/L)	61.0	293.0	152.0	55.7	36.7	-	-
DO (mg/L)	2.8	18.5	7.4	1.9	25.5	-	-
pH	7.2	9.4	8.0	0.4	5.2	6.5–8.5	4.2
EC (μS/cm)	446.0	7480.0	2025.0	1527.0	75.4	-	-
Temperature (°C)	9.8	24.8	14.3	2.9	20.4	-	-

Note: Al, aluminium; Mn, manganese; Fe, ferrum; Co, cobalt; Ni, nickel; Cu, copper; Zn, zinc; As, arsenic; Cd, cadmium; Pb, lead; TDS, total dissolved solids; DO, dissolved oxygen content; EC, electrical conductivity; SD, standard deviation; CV, coefficient of variation; Percentage of SER, percentage of samples exceeding permissible value. [#] represents the standard for Chinese drinking water (Ministry of Health of the People's Republic of China, 2006) and World Health Organization (WHO) standard (World Health Organization, 2011); "-" refers no data.

Table S2 Comparison of the average concentrations of heavy metal(loid)s in groundwater or river

Groundwater or river	Al (μg/L)	Mn (μg/L)	Fe (μg/L)	Co (μg/L)	Ni (μg/L)	Zn (μg/L)	As (μg/L)	Cd (μg/L)	Pb (μg/L)	Reference
Shule River Basin	3.5	0.4	358.0	0.2	4.0	5.7	1.6	0.0	0.1	This study
Rivers in NQTP	1753.0	5.6	76.7	0.3	2.4	35.2	3.4	0.2	3.0	Li et al. (2022)
Heihe River	10.5	2.6	187.0	-	-	-	0.8	<0.1	<0.1	Qu et al. (2019)
Buh River	18.2	3.8	198.0	-	-	-	0.9	N.D.	<0.1	Qu et al. (2019)
Yellow River	10.2	3.3	154.0	-	-	-	1.2	<0.1	0.1	Qu et al. (2019)
Za'gya Zangbo River	39.8	0.3	-	-	-	-	5.7	N.D.	0.0	Qu et al. (2019)
Yangtze River	-	30.7	-	1.9	2.8	20.5	-	3.6	15.8	Qu et al. (2017)
Lancang River (Mekong River)	14.8	1.7	2.6	-	-	-	-	-	-	Huang et al. (2009)
Salween River (Nujiang River)	20.7	-	19.7	-	-	-	-	-	-	Huang et al. (2009)
Yarlung Zangbo River	20.6	12.8	-	-	-	-	10.5	1.0	5.6	Qu et al. (2015) and Zheng et al. (2010)
Ganges River	<0.2	N.D.	0.4	-	-	-	N.D.	N.D.	N.D.	Zhang et al. (2015)
Indus River	<8.8	0.4	N.D.	-	-	-	13.7	N.D.	-	Zhang et al. (2015) and Qu et al. (2019)
Chinese Loess Plateau	18.1	58.2	67.0	7.3	13.2	46.8	15.2	0.0	0.5	Xiao et al. (2019)
Tarim River Basin	32.0	80.4	219.0	0.2	0.5	10.1	5.8	0.0	0.8	Xiao et al. (2014)
Zhangye Basin	3.6	6.3	181.0	0.1	2.5	1.9	1.3	0.0	0.1	Sheng et al. (2022)

Note: NQTP, northeastern Qinghai-Tibet Plateau; N.D., not detected; -, no data available.

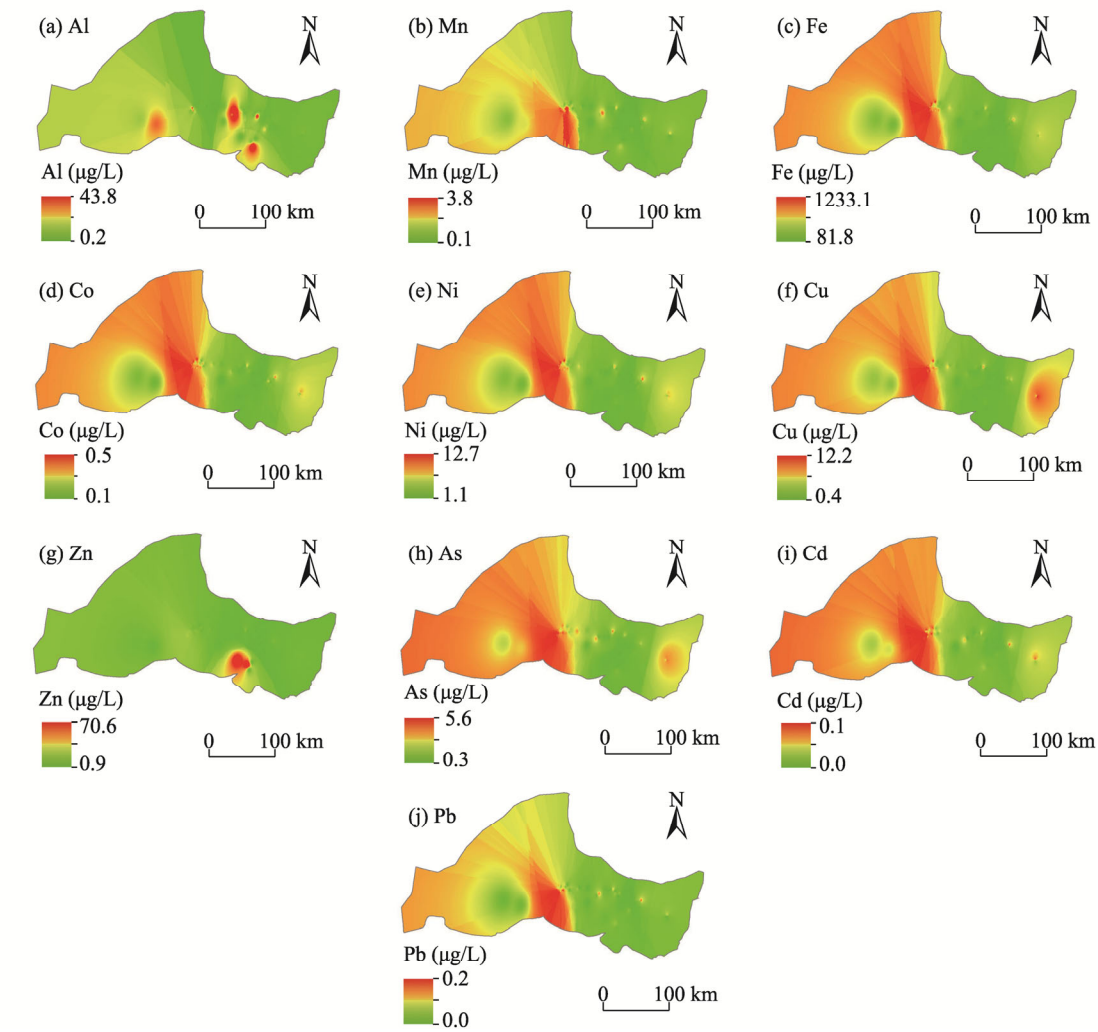

Fig. S1 Spatial distribution of the concentrations of heavy metal(loid)s in groundwater of the Shule River Basin. (a), aluminum (Al); (b), manganese (Mn); (c), ferrum (Fe); (d), cobalt (Co); (e), nickel (Ni); (f), copper (Cu); (g), zinc (Zn); (h), arsenic (As); (i), cadmium (Cd); (j), lead (Pb).

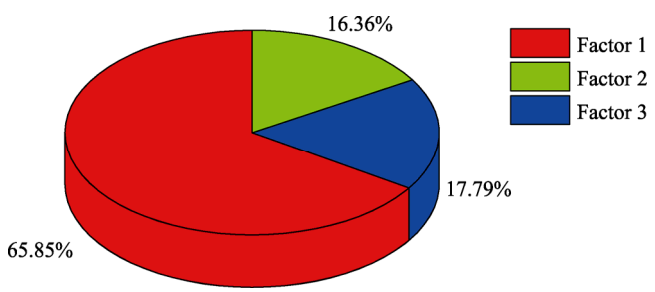

Fig. S2 Contributions from three sources by absolute principal component scores-multiple linear regression (APCS-MLR) model. Factor 1 represents human activities and the initial geological environment factor, Factor 2 represents industrial activity factor, and Factor 3 represents agricultural practices factor.

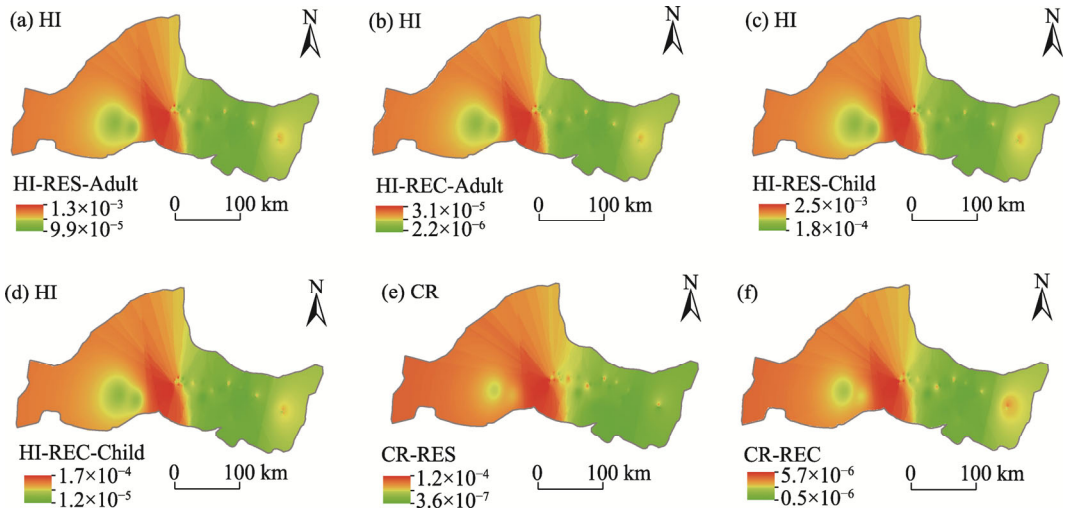

Fig. S3 Hazard index (HI; a–d) and carcinogenic risk (CR; e and f) from heavy metal(loid)s for residential and recreational (b, d and f) receptors in groundwater of the Shule River Basin. HI-RES-Adult, hazard index for residential adults; HI-REC-Adult, hazard index for recreational adults; HI-RES-Child, hazard index for residential children; HI-REC-Child, hazard index for recreational children; CR-RES, carcinogenic risk for residential receptors; CR-REC, carcinogenic risk for recreational receptors.

References

Huang X, Sillanpää M, Gjessing E T, et al. 2009. Water quality in the Tibetan Plateau: major ions and trace elements in the headwaters of four major Asian rivers. Science of the Total Environment, 407(24): 6242–6254.

Li L M, Wu J, Lu J, et al. 2022. Water quality evaluation and ecological-health risk assessment on trace elements in surface water of the northeastern Qinghai-Tibet Plateau. Ecotoxicological and Environmental Safety, 241: 10, doi: 10.1016/j.ecoenv.2022.113775.

Ministry of Health of the People's Republic of China. 2006. Standards for Drinking Water Quality (GB5749-2006). [2023-05-10]. https://std.samr.gov.cn/gb/search/gbDetailed?id=71F772D7FC82D3A7E05397BE0A0AB82A.

Qu B, Sillanpää M, Zhang Y L, et al. 2015. Water chemistry of the headwaters of the Yangtze River. Environmental Earth Sciences, 74(8): 6443–6458.

Qu B, Zhang Y L, Kang S C, et al. 2017. Water chemistry of the southern Tibetan Plateau: an assessment of the Yarlung Tsangpo river basin. Environmental Earth Sciences, 76(2): 74, doi: 10.1007/s12665-017-6393-3.

Qu B, Zhang Y L, Kang S C, et al. 2019. Water quality in the Tibetan Plateau: Major ions and trace elements in rivers of the "Water Tower of Asia". Science of the Total Environment, 649: 571–581.

Sheng D, Meng X H, Wen X H, et al. 2022. Contamination characteristics, source identification, and source-specific health risks of heavy metals in groundwater of an arid oasis region in Northwest China. Science of Total Environment, 841: 156733, doi: 10.1016/j.scitotenv.2022.156733.

World Health Organization. 2011. Guidelines for Drinking-water Quality. [2023-05-10]. https://www.who.int/publications/i/item/9789240045064.

Xiao J, Jin Z D, Wang J. 2014. Geochemistry of trace elements and water quality assessment of natural water within the Tarim River Basin in the extreme arid region, NW China. Journal of Geochemical Exploration, 136: 118–126.

Xiao J, Wang L Q, Deng L, et al. 2019. Characteristics, sources, water quality and health risk assessment of trace elements in river water and well water in the Chinese Loess Plateau. Science of the Total Environment, 650(2): 2004–2012.

Zhang Y L, Sillanpää M, Li C L, et al. 2015. River water quality across the Himalayan regions: elemental concentrations in headwaters of Yarlung Tsangbo, Indus and Ganges River. Environmental Earth Sciences, 73(8): 4151–4163.

Zheng W, Kang S C, Feng X B, et al. 2010. Mercury speciation and spatial distribution in surface waters of the Yarlung Zangbo River, Tibet. Chinese Science Bulletin, 55(24): 2697–2703.